Accepted Manuscript

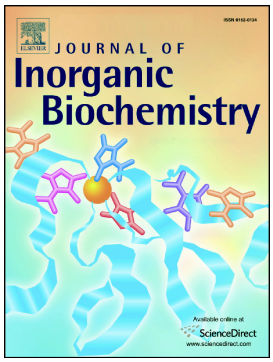

Chloro(triphenylphosphine)gold(I) a forefront reagent in gold chemistry as apoptotic agent for cancer cells

M.P. Chrysouli, C.N. Banti, N. Kourkoumelis, N. Panayiotou, A.J. Tasiopoulos, S.K. Hadjikakou

PII: S0162-0134(17)30461-0
DOI: doi:10.1016/j.jinorgbio.2017.11.004
Reference: JIB 10364

To appear in: *Journal of Inorganic Biochemistry*

Received date: 28 June 2017
Revised date: 30 October 2017
Accepted date: 4 November 2017

Please cite this article as: M.P. Chrysouli, C.N. Banti, N. Kourkoumelis, N. Panayiotou, A.J. Tasiopoulos, S.K. Hadjikakou , Chloro(triphenylphosphine)gold(I) a forefront reagent in gold chemistry as apoptotic agent for cancer cells. The address for the corresponding author was captured as affiliation for all authors. Please check if appropriate. Jib(2017), doi:10.1016/j.jinorgbio.2017.11.004

Chloro(triphenylphosphine)gold(I) a forefront reagent in gold chemistry as apoptotic agent for cancer cells

M.P. Chrysouli[a], C.N. Banti[a,*], N. Kourkoumelis[b], N. Panayiotou[c], A.J. Tasiopoulos[c], S.K. Hadjikakou[a,*]

[a] Inorganic and Analytical Chemistry, Department of Chemistry, University of Ioannina, 45110 Ioannina, Greece

[b] Medical Physics Laboratory, Medical School, University of Ioannina, Greece

[c] Department of Chemistry, University of Cyprus, 1678 Nicosia, Cyprus

*All correspondence should be addressed to:

Dr. C.N. Banti (Postdoctoral Fellow); email: cbanti@cc.uoi.gr

Dr. S.K. Hadjikakou (Professor); e-mail: shadjika@uoi.gr; tel. x30-26510-08374

fax +30-26510-08786

Abstract

The antiproliferative activity of the gold complex [Au(tpp)Cl] (**1**) against human breast adenocarcinoma cells (MCF-7) and normal human fetal lung fibroblast cells (MRC-5) was investigated. The compound exhibits stronger activity against MCF-7 cells than cisplatin. The apoptotic pathway, especially though the mitochondrion damage, was confirmed by cell cycle arrest and permeabilization of the mitochondrial membrane tests. The molecular mechanism of action of **1** was further studied by: (i) its catalytic activity on the oxidation of linoleic acid (an acid that partakes in membrane fluidity) to hyperoxolinoleic acid by oxygen and (ii) its binding affinity towards the calf thymus (CT) DNA. Since the deactivation of cisplatin by glutathione (GSH), is related with the development of cell resistance, the reaction of **1** with GSH was investigated by UV absorption spectroscopy. The absence of micronucleus in cells confirms that the complex has no *in vitro* toxicity. The *in vivo* genotoxicity caused by **1** was evaluated by *Allium cepa* test.

Keywords: Medicinal Chemistry; Metallotherapeutic; gold(I) complexes; breast cancer cells; pnictogen; apoptosis.

Introduction

Cancer is the second leading cause of death behind cardiovascular diseases, while over 8 million people worldwide are dying from cancer annually [1]. Breast cancer is the most frequent cause of cancer death among females worldwide. Platinum based anticancer drugs such as cisplatin, carboplatin and oxaliplatin has been approved by FDA and there are in clinic use for the treatment of various types of cancer [2]. However, the major barriers of platinum-based anticancer drugs are the side effects, toxicity and drug resistance. Thus, there is a need for development of new anticancer metallodrugs [3].

Among the new non-platinum drugs especially gold compounds have gained more attention [4]. Epidemiological, clinical and experimental studies show that gold metallodrugs are promising cancer chemotherapeutic agents [5]. The spectrum of gold complexes includes a variety of different ligands linked to gold, oxidation states +1 or +3 and different molecular structures. The most widely used gold compounds are complexes with phosphines and carbines, dithiocarbamates or porphyrinates [5-11].

Antitumor compounds activate apoptosis in cancer cell. One pathway for the achievement of apoptosis is through the dis-rupture of mitochondrial membrane, with the releasing of proapoptotic factors from mitochondria to cytoplasm, simultaneously [12]. A wide range of mitochondriotropic ligands (containing pnictogens) can be connected to specific metallotherapeutics and they are used for the targeted delivery of the drugs in to the mitochondria [13].

In the course of our studies towards the development of new metallotherapeutics [13-15], we investigate here the anticancer properties of the metallodrug chloro(triphenylphosphine)gold(I) ([Au(tpp)Cl] **(1)**). The chemical part of **1** is overdeveloped due to its great importance in gold(I) chemistry. A great number of gold(I) compounds are derived by the substitution of the Cl atom [16]. The medical applications of chloro(triphenylphosphine)gold(I), on the other hand, are weak investigated. Mirabelli, et.al reported earlier the *in vitro* cytotoxicity of **1** against both B16 melanoma cells and P388 leukemia **c**ells as well as its *in vivo* activity against P388 leukemia in

mice [4d,17]. Although, the high activity of gold(I) complexes has been related with their high lipoxygenase (LOX, an enzyme which oxidizes fatty acids to leukotriens and it is manly located in the mitochondrion) inhibitory activity [18], however, the exact mechanism of **1** against MCF-7 cells, still remains unknown. This is why we have undertaken to investigate the interaction of **1** against this type of tumour cells. By taken into account: (i) the high LOX inhibitory activity caused by **1** [18] and (ii) the antimitochondrial effects, such as mitochondrial swelling or increased permeability of the inner membrane caused by the (triethylphosphine)gold(I)chloride (TEPAuCl) an analogue of **1** [6], a strong antitumor activity is expected for **1.** This is because the presence of the mitochondriotropic ligand, triphenylphosphine, in the coordination sphere is expected to transfer the metal ion into mitochondria of breast cancer cells.

Compound **1** was characterized by melting point, IR, ^{1}H NMR, UV−vis spectra, and X-ray crystallography. Although the cytotoxic activity of 1 against cancer cell is known [4d,17] the clarification of its mechanism of action is studied for the first time here. Thus, the *in vitro* antiproliferative activity against breast adenocarcinoma cells, MCF-7 (ER positive) cell lines was tested. The evaluation of genotoxicity by micronucleus assay *in vitro* and Allium cepa test *in vivo* demonstrate no toxicity. The apoptotic pathway was tested by morphology studies, cell cycle arrest studies, and studies on the permeabilization of the mitochondrial membrane. Finally the molecular mechanism is elucidated by the mean of their interaction with the intracellular components: (i) calf thymus (CT) DNA, (ii) catalytic oxidation of the linoleic acid, (iii) GSH.

Results and Discussion:

General aspects: Tetrachloroauric(III) acid ($HAuCl_4$) solution was prepared according to the procedure reported previously by dissolving Au foil into a mixture of concentrated hydrochloric acid and nitric acid 4:1 [19]. Compound **1** and the ionic co-product **1a**, were formed by reacting $HAuCl_4$ with tpp in 1:2 molar ratio (Chart 1). Crystals of **1** were grown by slow evaporation of

diethyl ether solution which was used for the purification of the mixture. The ionic co-product **1a** is insoluble in the non polar media.

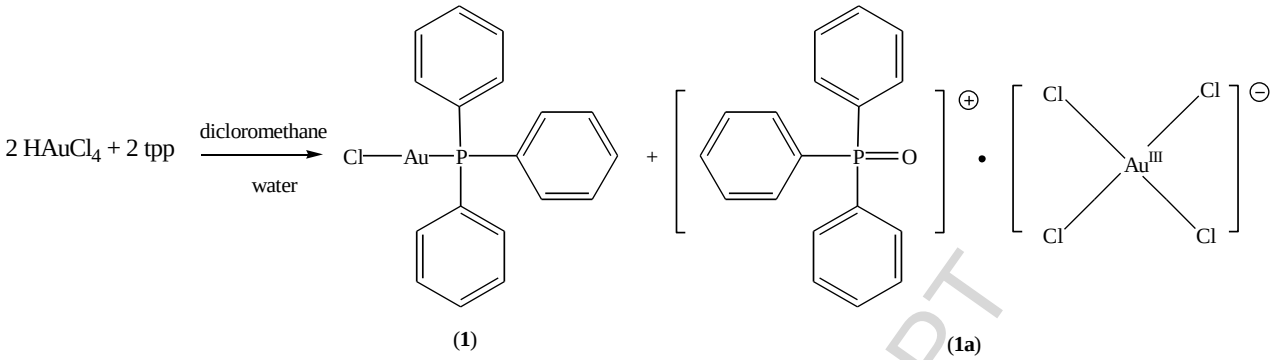

(**1**) (**1a**)

Chart 1

The formula of **1** was defined by spectroscopic methods. The crystal and molecular structure of **1** was determined by single crystal X-ray diffraction analysis. The structure of **1** was found to be identical with the already reported elsewhere [4d].

Solid state studies:

*Crystal and molecular structure of [Au(tpp)Cl] (**1**):* Although, the crystal structure of **1** is already known, however (i) the modification in the crystallization process of the drug followed here and (ii) the existence of two different polymorphs of the drug, prompt us to re-determinate the structure of **1**. The crystallographic parameters of the polymorphs are, **Polymorph A**: space group P212121, a= 12.300 (4), b= 13.084 (4), c=10.170 (3) A, α= 90, β=90, γ= 90^o, R=0.037 [20], **Polymorph B**: space group P1; a= 11.862(2), b= 10.921(3), c= 14.701(2) Å, α= 113.65(2), β= 99.35(3), γ= 109.31(3)^o; R= 0.041 [21]. The crystallographic parameters of **1** are: space group: orthorhombic P; a= 10.119, b= 12.340, c= 12.99 Å, α= 90, β=90, γ= 90^o, which categorize **1** in **polymorph A** type. Molecular diagram of **1** is shown in Figure 1.

Figure 1

Calculation of Hirshfeld volumes, intermolecular contacts and lipophilicity: In order to rationalize the bioactivity of **1** in structural terms, its Hirshfeld volume, inter-atomic contacts and lipophilicity are calculated. The Hirshfeld surface is defined as the volume of space where the molecule electron density exceeds that from all neighbouring molecules and provides a three-dimensional picture of the close contacts in a crystal structure [22a]. The calculated volume closed by Hirshfeld surface of **1** is 405.04 A^3, while the close contacts of all elements inside the area with the outer hydrogen atoms is 75.9 % for **1** (Table 1) [22b]. The lipophilicity (Log(P)) is expressed by their octanol–water partition coefficient and it is calculated based on the crystal structure. The Log(P) of **1** is 5.77 (Table 1). Table 1 summarizes structural data of gold(I) complexes of tpp among with their IC_{50} values.

Table 1

Vibrational spectroscopy: The *ν*(C-P) vibration bands of the triphenylphosphine at 492-514 cm^{-1} have been strongly shifted in the case of **1** at 507-544 cm^{-1}, indicating that the tpp has been coordinated to Au(I) ion though phosphorus atom (Figure S1).

Solution studies

The retention of the formulae in solution is confirmed by Uv-Vis study (Figure S2). No changes were observed between the initial UV spectrum and the corresponding spectrum when measured after 48 hrs. The period of at least 48 hrs for the stability testing of the complexes was chosen since biological experiments require 48 hrs incubation of the cell culture with complexes.

^{1}H-NMR studies: The aromatic protons of triphenylphopshine are observed at 7.378-7.173 ppm. These protons are shifted in the region of 7.380-7.253 ppm, in the case of **1** (Figure S3), indicating the coordination of tpp to the metal ion through its P atom.

Biological Tests

Anti-proliferative activity: Metallodrug **1** was tested for its *in vitro* antiproliferative activity against human breast adenocarcinoma cell line, MCF-7 by sulforhodamine B (SRB) assay [23].

The IC_{50} value of **1** against MCF-7 cells was measured, upon their incubation with multiple concentrations of **1** after 48 hrs and is summarized in Table 1 along with the IC_{50} values of tpp, tetrachloroauric acid and those of the known metallodrugs cisplatin and auranofin. Metallodrug **1** exhibits 1.5-fold stronger activity against MCF-7 cells (IC_{50}= 3.8±0.8 μM), than cisplatin (IC_{50}= 5.5±0.4 μM) and 3-fold higher than auranofin (IC_{50}= 13.1 μM) a gold(I) complex [24a]. Moreover, both the ligand tpp and the tetrachloroauric acid exhibit no activity against MCF-7 cells at the concentrations tested (up to 30 μM).

The toxicity of **1** against normal human fetal lung fibroblast cells (MRC-5 cells) was also evaluated. Compound, **1** exhibits similar toxicity against MRC-5 cells with cisplatin (1.3 towards 1.1 μM respectively), while auronofin (IC_{50}= 0.9 μM) shows higher toxicity than **1** [24a]. The tpp and tetrachloroauric acid have no toxicity against MRC-5 cells in the tested concentrations, up to 30 μM.

The therapeutic potency index (TPI) was also determined in order to study the selectivity of the agents against cancerous than normal cells. TPI is defined as the IC_{50} value against normal cells toward the corresponding IC_{50} value against cancerous cells of similar tissue [13]. The TPI value of **1** is 0.3, which classifies **1** into a potent antitumor agent with similar TPI value with cisplatin (0.2). Auronofin, on the other hand, exhibits lower TPI value (0.06), indicating strong toxic than antiproliferative activity.

Other gold(I) complexes of tpp, have already been studied for their anti-proliferative activity [24]. Thus, the gold compounds: [Au(6-ethoxy-9H-purine)(tpp)] (**2**), [Au(6-butyloxy-9H-purine)(tpp)] (**3**), [Au(6-allyloxy-9H-purine)(tpp)] (**4**), [Au(6-phenetyloxy-9H-purine)(tpp)] (**5**), [Au(2-chloro-6-ethoxy-9H-purine)(tpp)] (**6**), [Au(2-chloro-6-butyloxy-9H-purine)(tpp)] (**7**) and [Au(2-chloro-6-allyloxy-9H-purine)] (**8**), [Au(2-chloro-6-benzyloxy-9H-purine)(tpp)] (**10**),

AutppCH=CH(Br)-$C_{15}H_9NO_3$ (**11**), Autpp$(C_5H_4)_2$FeCH=CH-$C_{15}H_9NO_3$ (**12**), Autpp$C_{17}H_9O_2$ (**13**) show lower activity against MCF-7 cells, when they are compared to **1**, showing its better activity. Compound [Au(6-benzyloxy-9H-purine)(tpp)] (**9**), however, exhibits similar activity with **1**. Correlation between the biological effects (IC_{50}) with the sterical factors calculated based on the crystal structures (MW, Hirshfeld volumes, intermolecular contacts and lipophilicity) shows that: (i) the lower the molecular weight or the Hirshfeld volume are, the stronger the activity is and (ii) the higher the lipophilicity or the close contacts of all elements inside the area with the outer hydrogen atoms are, the stronger the activity are. This is probably due to the better permeability of the molecule through membranes because of the hydrogen bonds which the molecule is able to form.

Thus, chloro(triphenylphosphine)gold(I) a precursor of gold(I) compounds possess better activity than other gold(I) complexes of tpp derivatives. Moreover, the better candidate of the series should posses low MW, volume, and high lipophilicity and intermolecular contacts.

Evaluation of Genotoxicity

(A) Evaluation of Genotoxicity by Micronucleus Assay in vitro: Micronucleus assay is a reliable and a cheap technique to evaluate the appearance of genetic damage caused by exogenous factors, since it is used as a biomarker. The detection of micronucleus (MN) indicates mutagenic, genotoxic or teratogenic effect [25a]. In the presence of exogenous genotoxic factors, the MN is formed due to the metaphase-anaphase transition of the mitotic cycle. The appearance of MN is due to aneugenic (whole chromosome) or clastogenic (chromosome breakage) damage [25b].

In order to value the genotoxicity, cultured MRC-5 cells was treated by **1** at the concentration of IC_{50} value. The micronucleus frequency in the MRC-5 cells, without treatment is 0.8 % and 1.0 % after treatment with DMSO. When the cells were treated by **1** and cisplatin, the frequencies are increased up to 1.9 % and 1.6 %, respectively (Table 2, Figure 2), indicating, the low genotoxicity of **1** which is similar to that of cisplatin.

Table 2

Figure 2

(B) Evaluation of Genotoxicity by Allium Cepa test in vivo: The genotoxicity of **1** is also *in vivo* tested by *Allium Cepa* test. The *Allium cepa* test shows high correlation with mammal test systems and has been widely used to evaluate cytotoxic and mutagenic effects of several agents [26]. DNA damages, such as chromosome aberrations (CA), nuclear abnormalities (NA) and micronucleus (MN), can be estimated during mitosis. These alterations can indicate the genotoxic effect of an agent, since DNA damage at the chromosome level is an important event in carcinogenesis [26].

The mitotic index (MI) (%) is defined as the ratio between the cells undergoing mitosis to the cells not undergoing mitosis, in a population. The cytotoxicity levels of an agent can be determined by the increase or decrease of the MI.

The mitotic index (%) and DNA damages such as chromosomal aberrations (%), nuclear abnormalities (%) and micronucleus (%) are calculated when *Allium cepa* is treated with 3, 30 and 300 μM of **1** for 48 hrs (Figures 3-4). The range of the concentrations studied contains the IC_{50} value of **1** against cancerous cells.

The analysis of MI reveals decreasing of cell division index after incubation by **1** at the concentrations of 30 μM (3.7 %) and 300 μM (3.6 %) towards control cells (6.6 %) (Figure 4) However, the concentration of 3 μM seems to not affect the mitotic index. Thus, few cells of *A. cepa* are in the phases of mitosis when cells are incubated with **1** (30 or 300 μM), indicating that the cell division is significantly inhibited. In addition, the decrease of mitotic index caused by **1** at 300 μM was also associated with the appearance of CA (Figure 3). CA is increased from 0.5 % at untreated cells to 1.5 % at the concentration of 300 μM (Figure 4). However, this concentration is 100-fold higher than the IC_{50} value of **1** (3.8 μM). Therefore this study reveals that **1** causes no formation of MN or NA, compared to the negative control. Generally, the metallodrug in the concentration of IC_{50} value, posses no mutagenic or genotoxic effect.

Figures 3-4

Mechanism of Action: Since the metallodrug exhibits no *in vitro* or *in vivo* genotoxicity in the IC_{50} value, the mechanism of action of **1** against MCF-7 cells was investigated by (a) cell morphology studies, (b) cell cycle studies and (c) permeabilization of the mitochondrial membrane test. In addition, the molecular mechanism of action of **1** was further studied by its (i) catalytic activity on the oxidation of linoleic acid to hyperoxolinoleic acid, (ii) binding affinity toward the calf thymus DNA (CT-DNA) and (iii) its binding affinity to glutathione (GSH).

Cell Morphology Study: Cell morphology studies are useful for the determination of the type of the cell death. Cell morphological observations disclose important characteristics of apoptosis or necrosis. In order to reveal important morphological changes, MCF-7 cells were treated by **1** at concentration equal to its IC_{50} value for 48 hrs. The morphological observations performed by light microscopy. When MCF-7 cells were treated by **1** or cisplatin, abnormal morphology appears. Cells are shrunk and rounded; the cell contact was lost, resulting in the detachment of the cells from the plate. These morphological observations demonstrate the apoptotic type of cell death. The control cells and treated cells with DMSO showed normal morphology (Figure 5). Thus, morphological studies suggest that the MCF-7 cell viability upon treatment with **1** maybe due to apoptotic way of cell death. Similar observations in MCF-7 cells were made when they are incubated with cisplatin [13].

Figure 5

Cell Cycle Study: In order to confirm the apoptotic type of MCF-7 cells caused by the metallodrug **1**, cell cycle study was performed. DNA frequency histograms can be used to identify apoptotic

cells by the appearance of sub-G_1 in cell population [27a]. Thus a flow cytometric analysis was performed to determine the possible apoptotic effect of **1** against MCF-7 cells. MCF-7 cells were treated by **1** at concentration equal to IC_{50}, stained with propidium iodide and the amount of DNA at each cell cycle phase was analyzed by flow cytometry.

1.8 % of control cells (untreated cells) are distributed in sub-G_1 phase, 55.7 % in G_0/G_1, 10.4 % in S and 31.9 % in G_2/M phase (Figure 6). After incubation of the MCF-7 cells with **1**, a significant increase in the number of apoptotic cells in sub-G_1 phase (4.3 %) was observed towards the control group (1.8 %). The percentage of cells in S phase, was increased to 11.9 %, when they were treated by **1**. Thus, **1** suppress cell proliferation by inhibiting DNA synthesis and inducing S-phase cell cycle arrest. Similarly, the percentage of cells in the G_2/M phase when they are treated with **1**, is increased to 33.1 %. Therefore, **1** also causes cell arrest at G_2/M phase. Many anticancer agents [27b], among them cisplatin [13], cause cell cycle arrest at S and G_2/M phases.

Moreover, gold(I)-alkynyl chromones have been biologically examined in respect to induce apoptosis against breast adenocarcinoma cells. After, incubation of MCF-7 cells with the gold(I) complexes, the cells are accumulated in the G_2/M phase. It is also revealed an increase in the sub-G_1 peak, including hypo-diploid apoptotic cells [24a]. These findings show that gold(I) complexes induced apoptosis in cells acting with the same mechanism.

Figure 6

Permeabilization of the mitochondrial membrane test: Apoptosis is a genetically predetermined cell mechanism caused by several molecular pathways. One of the major apoptotic pathways in mammalian cells is the intrinsic pathway. The intrinsic apoptotic pathway is also called the mitochondrial pathway because of the essential involvement of mitochondria [28a]. Mitochondria are involved in caspase activation through the release of apoptotic factors that are normally located in the mitochondrial inter-membrane space. Therefore, mitochondrial permeability transition pore

(MMP) opens, causing the release of soluble proteins such as cytochrome c. Thus, mitochondria play a key role in activating apoptosis in mammalian cells [28b]. It is known, that metallo-agents affecting MMP may be employed in cancer therapy [28c]. Moreover, metal complexes with mitochondriotropic agents, such as triarylphosphines can interact with mitochondrion and induce the permeability of mitochondrial membrane [13,29].

In order to detect the loss of the mitochondrial membrane permeabilization, MCF-7 cells were exposed at concentration equal to IC_{50} values of **1** or cisplatin. The cationic hydrophobic mitochondrial potential dye accumulates in normal mitochondria, while in the treated cells with the metallodrug, MMP collapses and results in a decreased fluorescence, indicating apoptosis and the release of cytochrome c in the cytosol [13]. The observed percent decrease of fluorescence, at treated cells with **1**, is 16.4 %, while for the treated cells with cisplatin is 54.9 %. In conclusion, **1** induces cell death via apoptotic pathway, since it opens MMP similarly to cisplatin. These results are also supported by cell morphology studies and cell cycle arrest experiments.

*The Influence of **1** upon the Peroxidation of Linoleic Acid:* In order to confirm further the influence of **1** against mitochondrion, its interaction with linoleic acid was also studied. The catalytic peroxidation of linoleic acid may cause a damage of the cell membrane or mitochondrion membrane, since linoleic acid is an essential membrane component [30]. Thus the influence of metallodrug **1** on the oxidation of linoleic acid to hyperoxo linoleic acid was studied. Peroxidation of linoleic acid was evaluated in the absence and presence of **1**, recorded the absorbance of hyperoxolinoleic acid which is formed at 234 nm (ε= 25000 ($M^{-1}cm^{-1}$), as described previously [13].

Metallodrug **1** catalyzes the peroxidation of the linoleic acid at the tested concentrations of 4 and 8 μM of **1**. The initial slope (V_o) for the oxidation reaction of free linoleic acid at 25°C, is 0.66×10^{-6} s^{-1} [13]. The corresponding V_o values for the peroxidation of the linoleic acid in the presence of **1** (4 and 8 μM) are 2.3×10^{-6} s^{-1} and 5.0×10^{-6} s^{-1} respectively. Cisplatin also catalyzes

the peroxidation of the linoleic acid [13]. Consequently, metallodrug **1** and cisplatin act similarly, concerning their ability to oxidize the linoleic acid. As a result, **1** and cisplatin may cause cell death by affecting cellular and mitochondrial membranes. These results support the permeabilization of the mitochondrial membrane test and the study of the peroxidation of linoleic acid by LOX.

DNA Binding Studies: In order to investigate further the mechanism of action of **1**, the interaction with calf thymus DNA (CT-DNA) was examined by UV-visible absorption spectroscopy [31a]. Metallodrugs can bind to DNA through either covalent bonds and/or through non-covalent interactions, such as intercalative, electrostatic or binding of complexes towards DNA helix, to major or minor grooves [31b]. The binding mode of metallodrugs towards DNA is investigated by UV-visible absorption spectroscopy [31c]. Thus, hypochromism is attributed to the intercalated or electrostatic binding mode, while hyperchromism is assigned to the breakage of hydrogen bonds, which stabilized the secondary structure of DNA [31d].

A slight decrease in the absorption intensity (at λ_{max}= 258 nm) is observed upon the presence of **1** at various concentrations, with a constant concentration of DNA ([DNA]= 10^{-4} M)). The tested r values are 0.02, 0.07, 0.1, 0.12 (r= [complex]/[DNA]). The calculated percent of hypochromicity is 5.4 %, suggesting intercalation or electrostatic binding of **1** towards DNA (Figure S4).

The binding constant (K_b) of **1** towards CT-DNA was evaluated by monitoring the changes in absorbance of the UV spectra of metallodrug (50 μM) at 300-310 nm, with increasing concentration of CT-DNA (Figure S5). The K_b constant is obtained from the ratio of the slope to the y-intercept in plots [DNA]/($\varepsilon_a-\varepsilon_f$) versus [DNA] [31d]. The K_b value of **1** is 6×10^4 M^{-1}, indicating that the **1** can bind with low affinity towards DNA, in contrast to silver(I) metallodrugs [13, 14d,31d].

Molecular Docking Studies: In order to design novel selective inhibitors, the nature of DNA interaction with small molecules must be understood. The nucleic acid sequence specific

recognition mechanism is essential to many minor groove binding ligands [32a]. Moreover, metal complexes that resemble to cisplatin have anticancer properties inhibiting DNA replication and transcription [32b]. Although metal complexes are difficult to parametrize for theoretical DNA docking, literature shows that correct results are expected in the case of groove binding [32c]. The B-DNA structure used for this study was the dodecamer $d(CGCGATATCGCG)_2$ (PDB ID: 1DNE [32d]). Small molecules tend to dock to the minor groove [32e] and **1** is not an exception (Figure 7) in accordance to the experimental results (see above).

The structure with the lowest energy (-6.76 Kcal/mol) is located in the AATT/TTAA segment favoring binding to the central electronegative AT rich region. The compound is stabilized by significant hydrophobic interactions and π-π interactions among the phenyl groups and the bases rings (Figure S6).

Figure 7

*Reaction of complex **1** with GSH:* Glutathione (GSH) is an abundant tripeptide, (contained by cysteine, glycine, and glutamic acid), generated exclusively in the cytosol and pumped into mitochondria. GSH protects cells against reactive oxygen species (ROS) and is also involved in the detoxification of xenobiotic and endogenous agents [33a]. Moreover, it is known that GSH play an important role in multi-drug resistance [33b].

The interaction of **1** with GSH was studied by Uv-vis spectroscopy, in order to evaluate the possible resistance development against **1**. The UV spectra of solutions containing, concentrations of **1** (16.5 (A), 33 (B) and 66 (C) μM) and GSH (16.5 mM) in 100 mM Tris–HCl, pH 7.4, at 37^{o}C were measured for a period of 1-6 hrs (Figure 8)

The increase absorption intensity, at 260 nm, of the solutions with time is partially due to the reaction of **1** with GSH (formation of metal-sulphur bonds) and partially due to the oxidation of GSH alone (formation of the disulfide GSSG). However, the formation rate of disulfide GSSG is

slow, as a result, the concentration of alone GSH is assumed not to be changed much over the time course (Figure S7). The absorbance associated with GSH-**1** formation is obtained, by abstracting the absorbance due to the disulfide from the observed absorbance (Figure 9).

The initial rate and the order of the reaction between GSH and **1** was calculated as reported previously [33c-d]. Table 3 summarizes the initial rates for **1** and cisplatin.

At the tested concentrations of **1** with the presence of GSH, the absorbance at 260 nm is increased, indicating that the **1** interacts with GSH. The same trend is also observed in the case of cisplatin [33e]. Metallodrug **1** binds to GSH with higher initial slope than cisplatin [33e], indicating higher affinity towards the tripeptide than that of cisplatin. The order of the reaction of **1** and cisplatin is first order, indicating that both metallodrugs interact similarly with GSH.

Figures 8-9

Table 3

Conclusion

The chloro(triphenylphosphine)gold(I) is a forefront reagent in gold chemistry since the majority of the mixed ligand gold(I) complexes derived by substitution reaction of the chloride atom. However, the mechanism of its action against tumor cells, remains unknown. Compound **1** exhibits high activity against MCF-7 cells, higher than cisplatin. Its meaningless *in vitro* and *in vivo* genotoxicity gives advantage in the usage of **1** as anti-tumor agent. Chloro(triphenylphosphine)gold(I) induces cell death via apoptosis (cell cycle arrest). *In vitro* permeabilization of the mitochondrial membrane and the *ex vivo* catalytic oxidation of linoleic acid by **1** apoptosis might be proceeded through mitochondrion pathway. The mechanism through mitochondrion apoptotic pathway is also suggested since **1** exhibits high LOX inhibitory activity (LOX is an enzyme located in the mitochondrion) [18] and due to the content of the mitochodriotropic ligand of a pnictogen (tpp) [13].

In conclusion, **1** acts with similar manner to cisplatin and maybe a candidate for the development of new metallodrugs against breast cancer cells

Experimental

Materials and instruments: All solvents used were of reagent grade. Triphenylphosphine was purchased from Sigma-Aldrich, Merck and used without further purification. The tetrachloroauric(III) acid (HAuCl4) solution (0.51 M) was prepared by dissolving 1 g Au foil into 10 ml mixture of concentrated hydrochloric acid (12 M) and nitric acid (16 M) 4:1 [19]. Dulbecco's modified Eagle's medium, (DMEM), fetal bovine serum, glutamine and trypsin were purchased from Gibco, Glasgow, UK. Phosphate buffer saline (PBS), CT-DNA, propidium iodide and RNase A were purchased from Sigma-Aldrich. Dimethyl sulfoxide and boric acid were from Riedel-de Haen. Melting points were measured in open tubes with a Stuart Scientific apparatus and are uncorrected. IR spectra in the region of 4000-370 cm^{-1} were obtained from KBr discs, with a Perkin-Elmer Spectrum GX FT-IR spectrophotometer. The ^{1}H-NMR spectra were recorded on a Bruker AC 400 MHz FT-NMR instrument in DMSO-d_6 solution. A UV-1600 PC series spectrophotometer of VWR was used to obtain electronic absorption spectra. FACS Calibur flow cytometer (Becton Dickinson, San Jose, CA, USA) was obtained for the cell cycle.

*Synthesis and crystallization of **1**:*

The compound **1** was synthesized with a modified procedure than that described earlier [4d]. The procedure follows: Chloro(triphenylphosphine)gold(I) derived from the reaction between 1 mmol triphenylphosphine (0.262 g) with 0.5 mmol of $HAuCl_4$ solution (1 ml, 0.5 M) in 10 mL dichloromethane and 10 mL distilled water. The solution was stirred overnight and the next day, the dichloromethane phase was isolated and it condensed to dryness in vacuum. The powder was dissolved in diethylether. Pure crystals of **1** were grown from diethylether solution.

1: Yellow crystal, melting point: 230-235 °C; Elemental analysis found: C: 48.50; H: 3.32,; calculated for $C_{18}H_{15}AuClP$: C: 48.62; H: 3.26; IR (cm^{-1}), (KBr): 1586 w, 1479 w, 1434 s, 1312 w, 1179 w, 1102 s, 1026 w, 998 w, 748 s, 713 s, 693 vs, 546 vs, 501 vs, 445 w, 414 w, 394 w, 382 w; ^{1}H-NMR (ppm) in DMSO-d_6: 7.380-7.253 (m, aromatic); UV-vis (DMSO): λ= 264 nm (logε= 3.27)

X-ray Structure Determination: Intensity data for the crystals of **1** were collected on an Oxford Diffraction CCD instrument, using graphite monochromated Mo radiation (λ=0.71073 Å). Cell parameters were determined by least-squares refinement of the diffraction data from 25 reflections. All data were corrected for Lorentz-polarization effects and absorption [34a]. The structure was solved with direct methods with SHELXS97 [34b] and refined by full-matrix least-squares procedures on F^2 with SHELXL97 [34c]. All non-hydrogen atoms were refined anisotropically, hydrogen atoms were located at calculated positions and refined via the "riding model" with isotropic thermal parameters fixed at 1.2 (1.3 for CH_3 groups) times the Ueq value of the appropriate carrier atom.

Calculation of Hirshfeld volumes, intermolecular contacts and lipophilicity: The volumes of Hirshfeld surface and the intermolecular contacts were calculated with CrystalExplorer (Version 3.1) [35]. The lipophilicity study was performed using the Marvin software ver. 16.7.25.0 by ChemAxon release at 2016, based on the crystal structures.

Biological tests:

Solvents used: The biological experiments including assessment of the cell viability with SRB assay, cell morphology, cell cycle, micronucleus and the permebalization of mitochondrial membrane were carried in DMSO/DMEM solutions 0.01-0.3 % v/v DMSO in DMEM for the compound. Stock solution of **1** (0.01 M) in DMSO was freshly prepared and diluted with cell culture medium to the desired concentration. For DNA binding studies, the experiments carried in

DMSO/buffer solutions (0.00025-0.025 % v/v DMSO). For lipoxygenase inhibitor activation and the peroxidation of linoleic acid, the experiments carried in DMSO/ buffer solutions (0.0002-0.004 % v/v DMSO) for **1**.

SRB assay: Stock solution of **1**, (0.01M) in DMSO was freshly prepared and diluted in with cell culture medium to the desired concentration. For the experiments, cells were plated (100 μL per well) in 96-well flat-bottom microplates at various cell inoculation densities (MCF-7 and MRC-5: 6000 and 2000 cells/well respectively). The SRB assay was carried out as previously described [13].

Evaluation of Genotoxicity

(A) Micronucleus: MRC-5 cells were seeded (at a density of 2×10^4 cells/well) in glass coverslips which were afterwards placed in six-well plates, with 3 mL of cell culture medium and incubate for 24 hrs. MRC-5 cells exposed with **1** in IC_{50} value for a period of 48 hrs. The number of micronucleated cells per 1000 cells was determined. The test was performed in accordance with the previous reported method [13].

(B) Allium Cepa test: Small bulbs (1.5–2.0 cm in diameter) of the common onion, *Allium cepa*, were purchased from a local market. Bulbs of *Allium cepa* were placed in test tubes (10 mL) which were filled with water and placed in the incubator at 25 °C, 50–60% humidity and 12 h/day lighting for 48 h. Aliquots from complex stock solutions (0.01 M in DMSO) were added in the test tubes to incubate the bulbs with the complexes, at 3, 30, and 300 μM. Onion bulbs (two per dose) were exposed to **1** for 48 hrs. The roots growing in double distilled water were used as a control. In order to evaluate the rate of the cellular division the microscopic parameter of the mitotic index was determined. All categories were analyzed by counting 1800 cells per concentration (300 cells per slide, total of six slides). The *Allium Cepa* test was carried out as previously described [15a].

Cell morphology Study: MCF-7 cells morphology of was observed under an inverse microscope, after incubation of MCF-7 cells by **1**, for 48 hrs.

Cell cycle Study: MCF-7 cells were seeded at a density of 10^5 cells/well in six-well plates at 37˚C for 24 hrs. Cells were treated with **1** at the IC_{50} value for 48hrs. The cells analysed by flow cytometry using a FACS Calibur flow cytometer (Becton Dickinson, San Jose, CA, USA). For each sample, 10000 events were recorded. The resulting DNA histograms were drawn and quantified using the FlowJo software (version FlowJo X 10.0.7r2) [27b].

Permeabilization of the mitochondrial membrane test: MCF-7 cells were treated with **1** at IC_{50} value. After 48 hrs of incubation period of **1**, the cell medium was removed and added the Dye Loading Solution. The cells were incubated in 5% CO_2 at 37° C for 30 minutes. Afterwards, 50 μl of Assay Buffer B is added of each well and are incubated for 30 minutes. The fluorescence intensity is measured at λ_{ex}= 540 and λ_{em}= 590 nm. The MMP assay kit used was purchased from sigma Aldrich "Mitochondria Membrane Potential Kit for Microplate Readers, MAK147".

*The Influence of **1** upon the Peroxidation of Linoleic Acid:* These studies were performed as previously reported [13].

DNA binding Studies: This study was carried out as described previously [31d].

*Reaction of complex **1** with GSH:* This study was carried out as described previously [33e].

Acknowledgementss

(i) CNB and SKH acknowledge the Oncology Department of Novartis Hellas S.A.C.I. for the financial support (project number: 81939) (ii) M.P.C., CNB and SKH would like to thank the Unit of bioactivity testing of xenobiotics, the University of Ioannina, for providing access to the facilities. (iii) M.P.C., CNB and SKH would like to thank the Atherothrombosis Research Centre of the University of Ioannina for providing access to the flow cytometer.

References

[1] D.M. Parkin, F. Bray, J. Ferlay, P. Pisani, Ca-Cancer J. Clin. 2005, 55, 74−108.

[2] B. Rosenberg, L.V. Camp, T. Krigas, Nature, 1965, 205, 698–699

[3] L. Kelland, Nat Rev Cancer, 2007, 7, 573–584

[4] (a) C. Schmidt, B. Karge, R. Misgeld, A. Prokop, R. Franke, M. Brönstrup, I. Ott, Chem. Eur. J., 2017, 23, 1869–1880; (b) V. Andermark, K. Göke, M. Kokoschka, M.A. Abu el Maaty, C. Tung Lum, T. Zou, R. Wai-Yin Sun, E. Aguiló, L. Oehninger, L. Rodríguez, H. Bunjes, S. Wöl, C.-M. Che, I. Ott, J. Inorg. Biochem., 2016, 160, 140-148; (c) L. Massai, D. Cirri, E. Michelucci, G. Bartoli, A. Guerri, M.A. Cinellu, F. Cocco, C. Gabbiani, L. Messori, Biometals, 2016, 29, 863–872; (d) (a) K.N. Kouroulis, S.K. Hadjikakou, N. Kourkoumelis, M. Kubicki, L. Male, M. Hursthouse, S. Skoulika, A.K. Metsios, V.Y. Tyurin, A.V. Dolganov, E.R. Milaeva, N. Hadjiliadis, Dalton Trans. 2009, 10446–10456

[5] S. Berners-Price, P.J. Barnard, 2014, Therapeutic gold compounds. In T. Storr (Ed.), Ligand Design in Medicinal Inorganic Chemistry (pp. 227–256). United Kingdom: John Wiley and Sons.

[6] I. Ott, Coord Chem Rev, 2009, 253, 1670–1681

[7] S.J. Berners-Price, A. Filipovska, Metallomics, 2011, 9, 863-73

[8] R. Rubbiani, I. Kitanovic, H.Alborzinia, S. Can, A. Kitanovic, L.A. Onambele, M. Stefanopoulou, Y. Geldmacher, W.S. Sheldrick, G. Wolber, A. Prokop, S. Wolfl, I. Ott, J. Med. Chem., 2010, 53, 8608–8618

[9] J.Darc S. Chaves, L. Guimaraes Tunes, C. Hebert de J. Franco, T. Martins Francisco, C. Cimini Correa, S.M.F. Murta, R.Lima Monte-Neto, H. Silva, A. Paula S. Fontes, M.V. de Almeida, Eur. J. Med. Chem., 2017, 127, 727-739

[10] P. Štarha, Z.Trávnícek, B. Drahoš, Z. Dvorák, Int. J. Mol. Sci., 2016, 17, 2084-2101

[11] F. Caruso, M. Rossi, J. Tanski, C. Pettinari, F. Marchetti, J. Med. Chem., 2003, 46, 1737-1742

[12] S. Fulda, L. Galluzzi, G. Kroemer, Nature Rev Drug Discov, 2010, 9, 447–464

[13] C.N. Banti, C. Papatriantafyllopoulou, M. Manoli, A.J. Tasiopoulos, S.K. Hadjikakou, Inorg. Chem., 2016, 55, 8681–8696

[14] (a) C.N. Banti, N. Kourkoumelis, C.G. Tsiafoulis, S. Skoulika, S.K. Hadjikakou, Polyhedron, 2017, 121, 115-122, (b) C.N. Banti, D.C. Charalampou, N. Kourkoumelis, A.M. Owczarzak, M. Kubicki, S.K. Hadjikakou, N. Hadjiliadis, Polyhedron, 2015, 87, 251-258, (c) E.I. Gkaniatsou, C.N. Banti, N. Kourkoumelis, S. Skoulika, M. Manoli, A.J. Tasiopoulos, S.K. Hadjikakou, J Inorg Biochem, 2015, 150, 108-119, (d) C.N. Banti, A.D. Giannoulis, N. Kourkoumelis, A.M. Owczarzak, M. Kubicki, S.K. Hadjikakou, J. Inorg. Biochem., 2015, 142, 132–144, (e) I.I. Ozturk, S. Yarar, C.N. Banti, N. Kourkoumelis, M.P. Chrysouli, M. Manoli, A.J. Tasiopoulos, S.K. Hadjikakou, Polyhedron, 2017, 123, 152-161,

[15] (a) M. Poyraz, S. Demirayak, C.N. Banti, M.J. Manos N. Kourkoumelis and S.K. Hadjikakou, J. Coord. Chem., 2016, 69, 3560-3579, (b) V.I. Balas, C.N. Banti, N. Kourkoumelis, S.K. Hadjikakou, G.D. Geromichalos, D. Sahpazidou, L. Male, M.B. Hursthouse, B. Bednarz, M. Kubicki, K. Charalabopoulos, N. Hadjiliadis, Aust. J. Chem., 2012, 65, 1625–1637, (c) D.B. Shpakovsky, C.N. Banti, E.M. Mukhatova, Y.A. Gracheva, V.P. Osipova, N.T. Berberova, D.V. Albov, T.A. Antonenko, L. Aslanov, E.R. Milaeva, S.K. Hadjikakou, Dalton Trans., 2014, 43, 6880-6890, (d) C.N. Banti, A.D. Giannoulis, N. Kourkoumelis, A. Owczarzak, M. Kubicki, S.K. Hadjikakou, Dalton Trans. 2014, 43, 6848-6863, (e) I.I. Ozturk, C.N. Banti, N. Kourkoumelis, M. Manoli, A.J. Tasiopoulos, A.M. Owczarzak, M. Kubicki, S.K. Hadjikakou, Polyhedron, 2014, 79, 151-160

[16] (a) P.J. Barnard, S. Berners-Price, Coord. Chem. Rev., 2007, 251, 1889–1902, (b) S. Berners-Price, R. Bowen, P. Galettis, P. Healy, M. McKeage, Coord. Chem. Rev., 1999, 185-186, 823–836

[17] C.K. Mirabelli, R.K. Johnson, D.T. Hill, L.F. Faucette, G.R. Girard, G.Y. Kuo, C. Mei Sung, S.T. Crooke, J. Med. Chem., 1986, 29, 218-223

[18] E. Georgiou, A. Metsios, N. Kourkoumelis, S. Karkabounas, K. Charalabopoulos, A. Badeka, S.K. Hadjikakou, J Enzyme Inhib Med Chem, 2011, 26, 592-597

[19] B.P. Block, Inorg. Synth. 1953, 4, 14

[20] N.C. Baenziger, W.E. Bennett, D.M. Soboroff, Acta Cryst. 1976, B32, 962-963

[21] M. Khan, C. Oldham, D.G. Tuck, Can. J. Chem. 1981, 59, 2714–2718

[22] (a) M.A. Spackman, D. Jayatilaka, CrystEngComm, 2009, 11, 19–32, (b) H.F. Clausen, M.S. Chevallier, M.A. Spackman, B.B. Iversen, New J. Chem., 2010, 34, 193–199

[23] (a) P. Skehan, R. Storeng, D. Scudiero, A. Monks, J. McMahon, D. Vistica, J.T. Warren, H. Bokesch, S. Kenney, M.R. Boyd, J Natl Cancer Inst, 1990, 82, 1107-1112, (b) V. Vichai, K. Kirtikara, Nat. Protoc. 2006, 1, 1112−1116

[24] (a) P. Hikisz, Ł. Szczupak, A. Koceva-Chyła, A. Guspiel, L. Oehninger, I. Ott, B. Therrien, J. Solecka, K. Kowalski, Molecules, 2015, 20, 19699–19718, (b) R. Krikavova, J. Hosek, J. Vanco, J. Hutyra, Z. Dvorak, Z. Travnicek, PLoS One, 2014, 9, e107373, (c) E.R.T. Tiekink, Crit Rev Oncol Hematol, 2002, 42, 225–248

[25] (a) M.L. Dis. Markers, 2014, 956835, (b) M. Fenech, Methods Mol Biol, 2008, 410, 185-216

[26] D.M. Leme, M.A. Marin-Morales, Mutat. Res., 2009, 682, 71–81

[27] (a) X. Huang, H.D. Halicka, F. Traganos, T. Tanaka, A. Kurose, Z. Darzynkiewicz, Cell Prolif., 2005, 38, 223–243, (b) S.H. van Rijt, I. Romero-Canelon, Y. Fu, S.D. Shnyder, P.J. Sadler, Metallomics, 2014, 6, 1014-1022

[28] (a) C. Wang, R. Youle, Annu Rev Genet, 2009, 43, 95–118, (b) P. Parone, M. Priault, D. James, S.F. Nothwehr, J.C. Martinou, Essays Biochem, 2003, 39, 41-51, (c) G. Kroemer, L. Galluzzi, C. Brenner, Physiol Rev, 2007, 87, 99-163

[29] M. Han, M.R. Vakili, H. Soleymani Abyaneh, O. Molavi, R. Lai, A. Lavasanifar, Mol. Pharmaceutics, 2014, 11, 2640−2649

[30] R.A. Vaughan, R. Garcia-Smith, M. Bisoffi, C.A. Conn, K.A Trujillo, Lipids Health Dis., 2012, 11, 142−152

[31] (a) T. Afrati, A.A. Pantazaki, C. Dendrinou-Samara, C. Raptopoulou, A. Terzis, D.P. Kessissoglou, Dalton Trans. 2010, 39, 765–7750, (b) F. Dimiza, F. Perdih, V. Tangoulis, I. Turel, D.P. Kessissoglou, G. Psomas, J. Inorg. Biochem., 2011, 105, 476–489, (c) E.C. Long, J.K. Barton, Acc. Chem. Res. 1990, 23, 271–273, (d) C.N. Banti, A.D. Giannoulis, N. Kourkoumelis, A.M. Owczarzak, M. Poyraz, M. Kubicki, K. Charalabopoulos, S.K. Hadjikakou, Metallomics, 2012, 4, 545–560

[32] (a) R. Schley, Science, 1988, 241, 1182-1187, (b) C.X. Zhang, S.J. Lippard, Curr. Opin. Chem. Biol., 2003, 7, 481-489, (c) C.G. Ricci, P.A. Netz, J. Chem. Inf. Model., 2009, 49, 1925-1935, (d) M. Coll, J. Aymami, G.A. van der Marel, J.H. van Boom, A. Rich, A.H. Wang, Biochemistry, 1989, 28, 310-320, (e) N. Shahabadi, M. Maghsudi, Mol. BioSyst., 2014, 10, 338-347

[33] (a) G. Wu, Y.Z. Fang, S. Yang, J.R. Lupton, T.D. Turner, J Nutr., 2004, 134, 489-492, (b) C. Syng-Ai, A. Leela Kumari, A. Khar, Mol. Cancer Ther., 2004, 3, 1101-1108, (c) J.C. Dabrowiak, J. Goodisman, A.-K. Souid, Drug Metab Dispos, 2002, 30, 1378-1384, (d) A. Halamikova, P. Heringova, J. Kasparkova, F.P. Intini, G. Natile, A. Nemirovski, D. Gibson, V. Brabec, J Inorg Biochem., 2008, 102, 1077-1089, (e) C.N. Banti, L. Kyros, G.D. Geromichalos, N. Kourkoumelis, M. Kubicki, S.K. Hadjikakou, Eur. J. Med. Chem., 2014, 77, 388-399

[34] (a) CrysAlis RED, version 1.171.31.5; Oxford Diffraction Ltd., 2006 (release 28-08-2006 CrysAlis171.NET), Oxford Diffraction, Crysalis CCD and Crysalis RED, Version p171.29.2, Oxford Diffraction Ltd, Abingdon, Oxford, England, 2006, (b) G.M. Sheldrick, Phase annealing in SHELX-90: direct methods for larger structures, Acta Crystallogr. A, 1990, 46, 467, (c) G.M. Sheldrick, SHELXL-97, Program for the Refinement of Crystal Structures, University of Göttingen: Göttingen, Germany, 1997

[35] S.K. Wolff, D.J. Grimwood, J.J. McKinnon, M.J. Turner, D. Jayatilaka, M.A. Spackman, CrystalExplorer (Version 3.1), University of Western Australia, 2012

Figure Captions

Figure 1. Molecular diagram together with the numbering scheme of **1** compound.

Figure 2. Representative pictures with micronucleus formed in MRC-5 cells treated with IC_{50} values of **1** and cisplatin for a period of 48 hrs; arrow indicates micronucleus in MRC-5 cells.

Figure 3. *Allium cepa* meristematic cells exposed to **1**. (A) Normal prophase, metaphase and anaphase in untreated *Allium cepa* meristematic cells. (B) Normal prophase and metaphase in *Allium cepa* meristematic cells incubated with DMSO.(C) *Allium cepa* meristematic cells exposed with 3 μM of **1**. Normal prophase and telophase. (D) *Allium cepa* meristematic cells exposed with 30 μM of **1**. Normal prophase and anaphase. (E) *Allium cepa* meristematic cells exposed with 300 μM of **1**. Chromosome aberration, prophase with chromosome adherence. (F) *Allium cepa* meristematic cells exposed with 300 μM of **1**. Chromosomes aberrations, anaphase with loss observed and metaphase with chromosome bridge.

Figure 4. The mitotic index % (MI), the chromosomal aberrations (%), the nuclear abnormalities (%) and the micronucleus (%) observed when *Allium cepa* incubated with **1** (3, 30, 300 μM).

Figure 5. Changes in the morphology of MCF-7 cells incubated with **1** and DMSO for 48 hrs has examined by phase contrast microscopy.

Figure 6. Effect of metallodrug **1** on cell cycle against MCF-7 cells. The relative number of cells within each cell cycle was determined by flow cytometry. Number of cells in sub-G_1, G_0/G_1, S and G_2/M phase are indicated.

Figure 7. Minor groove docking for **1**

Figure 8. UV spectra of the solutions (final volume of 2.0 ml) containing different concentrations of **1**; 16.5 (A), 33 (B) and 66 (C) μM in 100 mM Tris–HCl, pH 7.4

with a high excess of GSH (16.5 mM) (ratio: 1/1000, 1/500, 1/250 respectively) at 37 ^{o}C and the corresponding after 0–6 hrs.

Figure 9 Absorbance at 260 nm for **1** incubated with GSH (16.5 mM) in 100 mM Tris–HCl, pH 7.4, buffer containing 5 mM NaCl at 37 ^{o}C vs. time (0–6 hrs) (■), GSH (▲), the points derived from the subtraction among them (D curve) (♦), the absorbance of the complex **1** without GSH (●).

Table 1. Steric data (Hirshfeld surface volumes, intra-molecular contacts), molecular weight, lipophilicity (Log(P)) and bioactivity data (IC_{50} μM) recorded for **1** and gold metallodrugs against MCF-7 cells and MRC-5 cells

Compounds	**Volume** (A^3)	**Contacts** (%)	**MW**	**LogP**	**IC_{50} μM)**		**TPI**	**Ref.**
					MCF-7	**MRC-5**		
1	405.04	75.9	494.71	3.8	3.8±0.8	1.3±0.06	0.3	*
cisplatin			300.01	0.04	5.5±0.4	1.1±0.2	0.2	[15a]
tpp			262.29		28.9±1.4	>30	-	[13]
auronofin			679.49		13.1±0.9	0.9	0.06	[24a]
Chloroauric acid			339.76		>30	>30	-	*
[Au(6-ethoxy-9H-purine)(tpp)] (**2**)	551.19	74.6	622.39	5.264	15.2			[24b]
[Au(6-butyloxy-9H-purine)(tpp)] (**3**)			650.44		27.1			[24b]
[Au(6-allyloxy-9H-purine)(tpp)] (**4**)	560.21	74.3	634.41	5.732	12.4			[24b]
[Au(6-phenetyloxy-9H-purine)(tpp)] (**5**)			698.48		6.3			[24b]
[Au(2-chloro-6-ethoxy-9H-purine)(tpp)] (**6**)			656.84		5.2			[24b]
[Au(2-chloro-6-butyloxy-9H-purine)(tpp)] (**7**)			684.89		>50			[24b]
[Au(2-chloro-6-allyloxy-9H-purine)] (**8**)			668.85		>25			[24b]
[Au(6-benzyloxy-9H-purine)(tpp)] (**9**)			684.46		3.6			[24b]
[Au(2-chloro-6-benzyloxy-9H-purine)(tpp)] (**10**)			718.91		>25			[24b]
Autpp$CH{=}CH(Br)$-$C_{15}H_9NO_3$ (**11**)			792.38		5.5±0.7			[24a]
Autpp$(C_5H_4)_2FeCH{=}CH$-$C_{15}H_9NO_3$ (**12**)	1043.11	74.8	923.53	4.231	11.0±0.8			[24a]
Autpp$C_{17}H_9O_2$ (**13**)	684.71	71.4	704.48	7.099	13.0±2.3			[24a]

* this work

Table 2. Percentage of micronucleus of **1** and cisplatin after the treatment of MRC-5 cells

	Percentage of micronucleus (%)
Control	0.8
DMSO	1.0
1	1.9
Cisplatin	1.6

Table 3. Initial rates of the reactions between **1**, cisplatin and GSH obtained from UV absorption data at 260 nm as a function of time (0-360 min). The differences were fitted to the equation: $I_d = C + A_1 \exp(-b_1 t) + A_2 \exp(-b_2 t)$, while the initial slope (S_{in}) was calculated as $-(A_1 b_1 + A_2 b_2)$.

1 (μM)	Glutathione (mM)	Initial slope $\times 10^{-3}$ (min^{-1})	R^2
16.5	16.5	0.243965	0.906
33.0	16.5	1.649433	0.974
66.0	16.5	1.94781	0.995
Cisplatin (μM) [33e]			
33.0	16.5	0.363546	0.996
66.0	16.5	0.798089	0.998

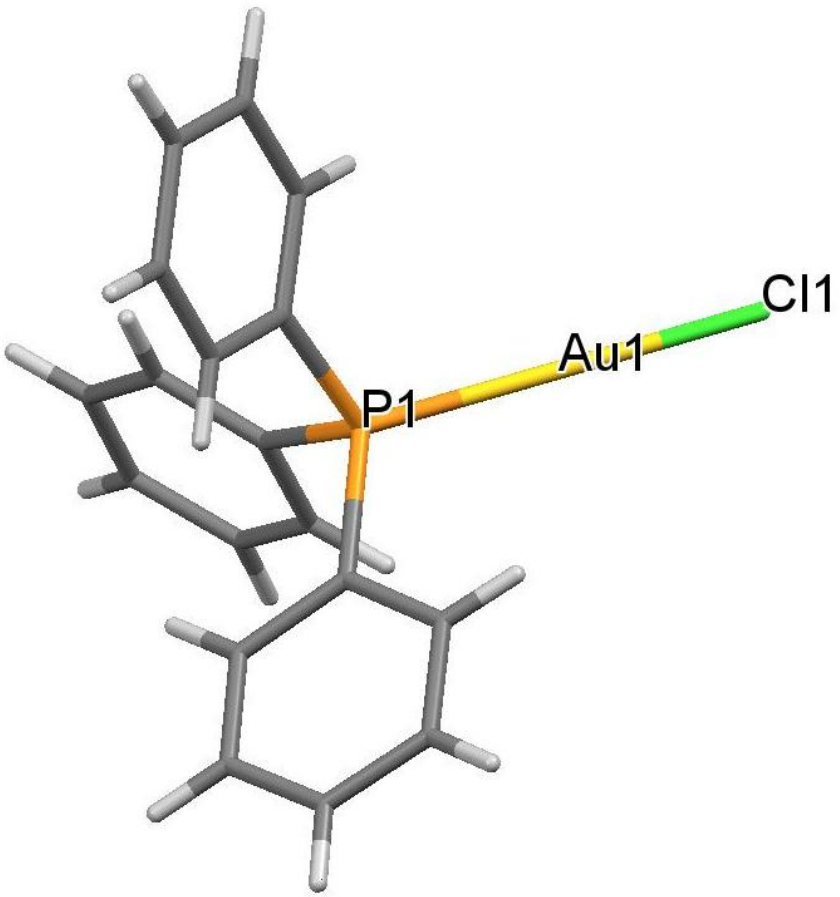

Figure 1

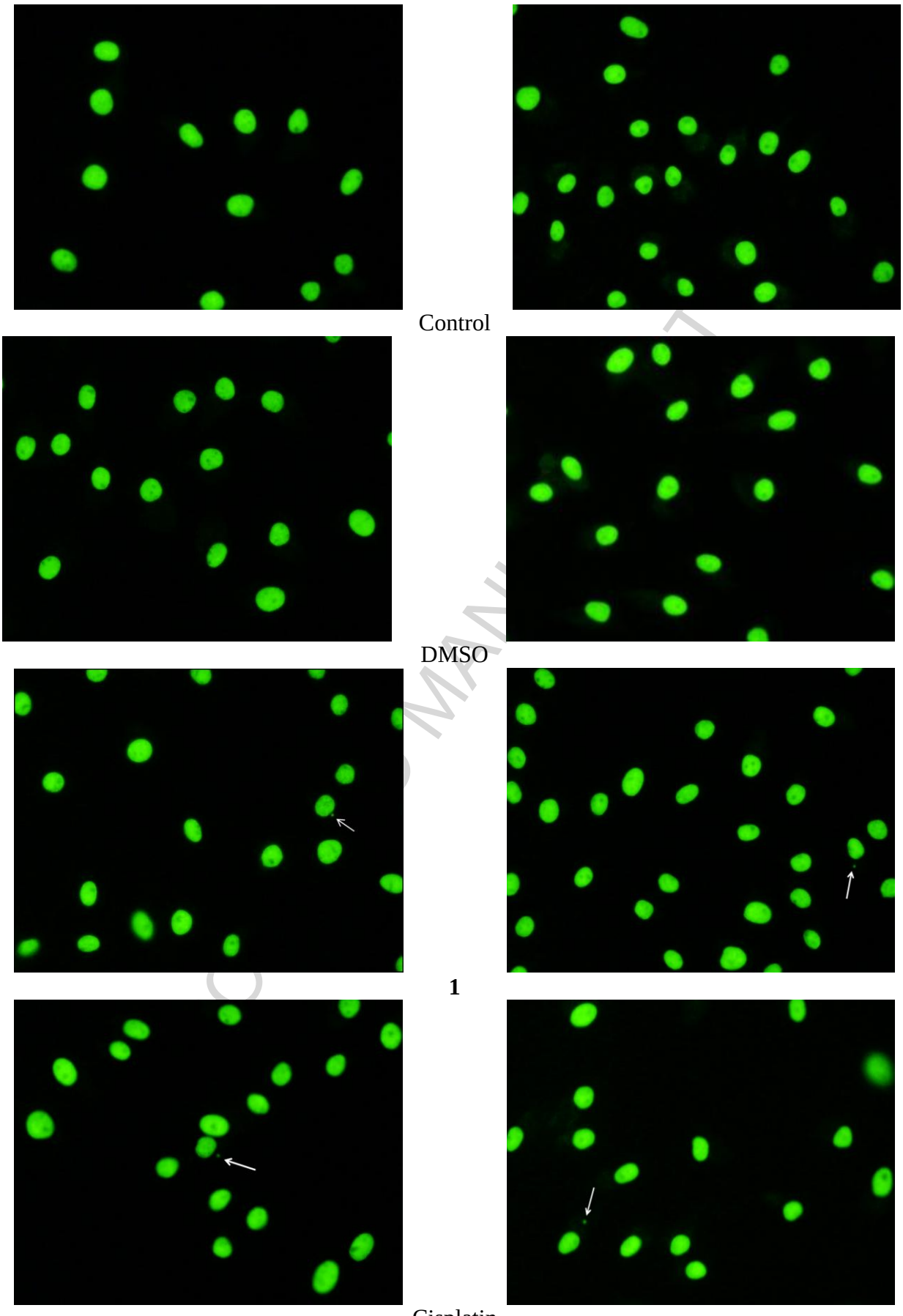

Figure 2

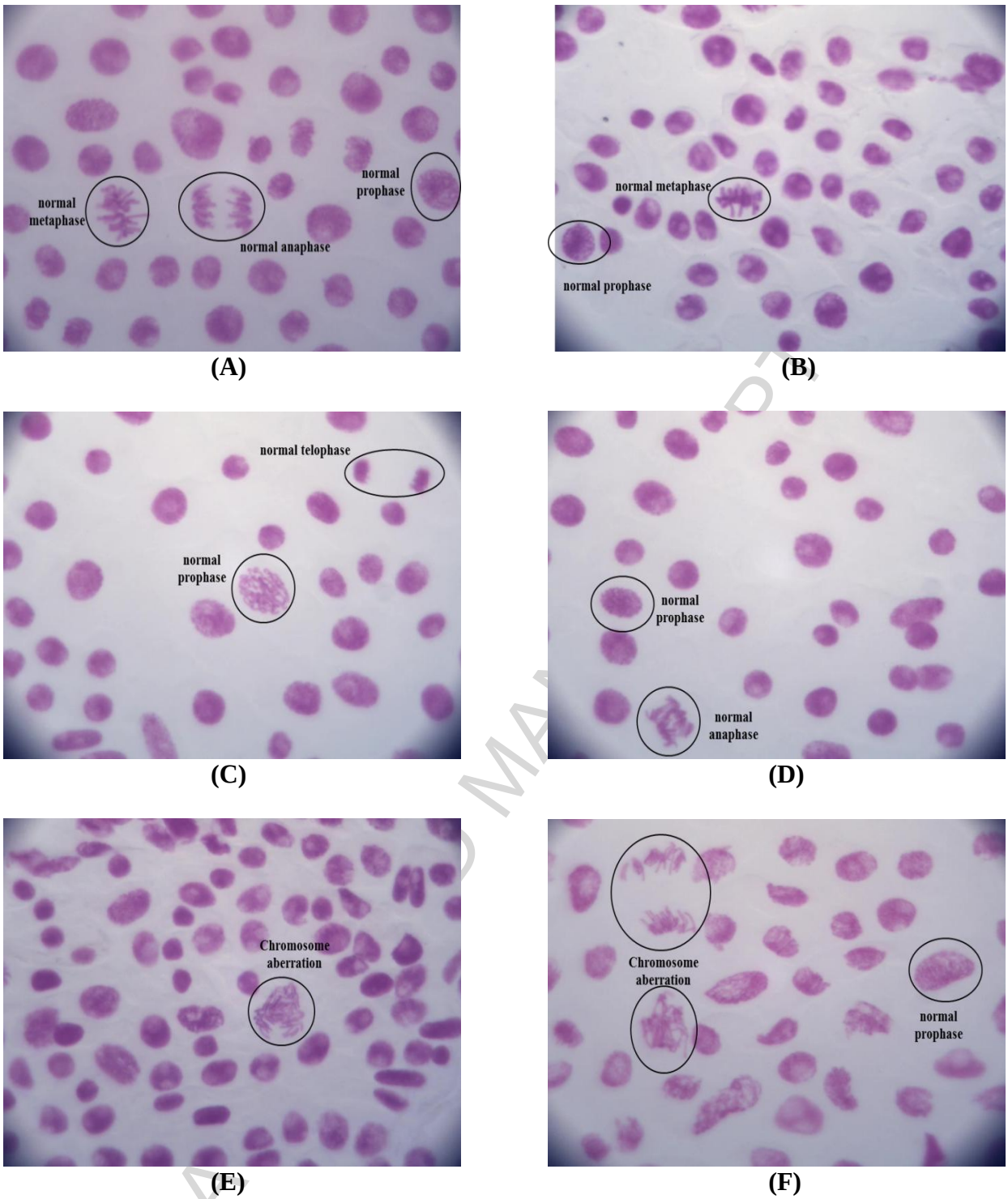

Figure 3

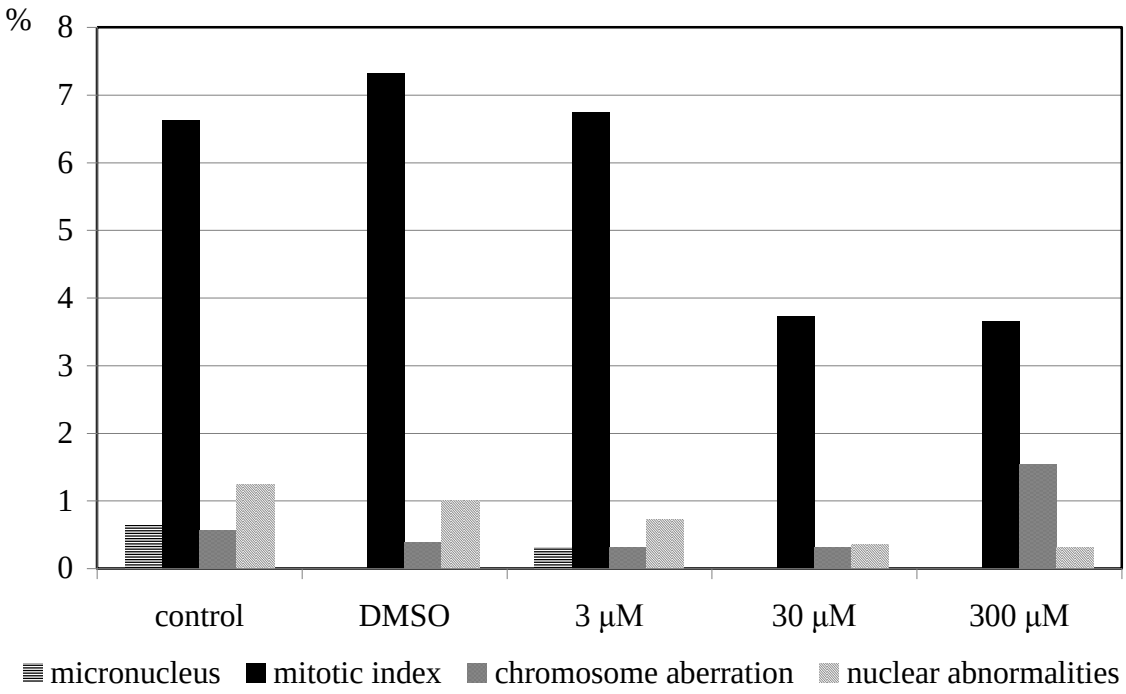

Figure 4

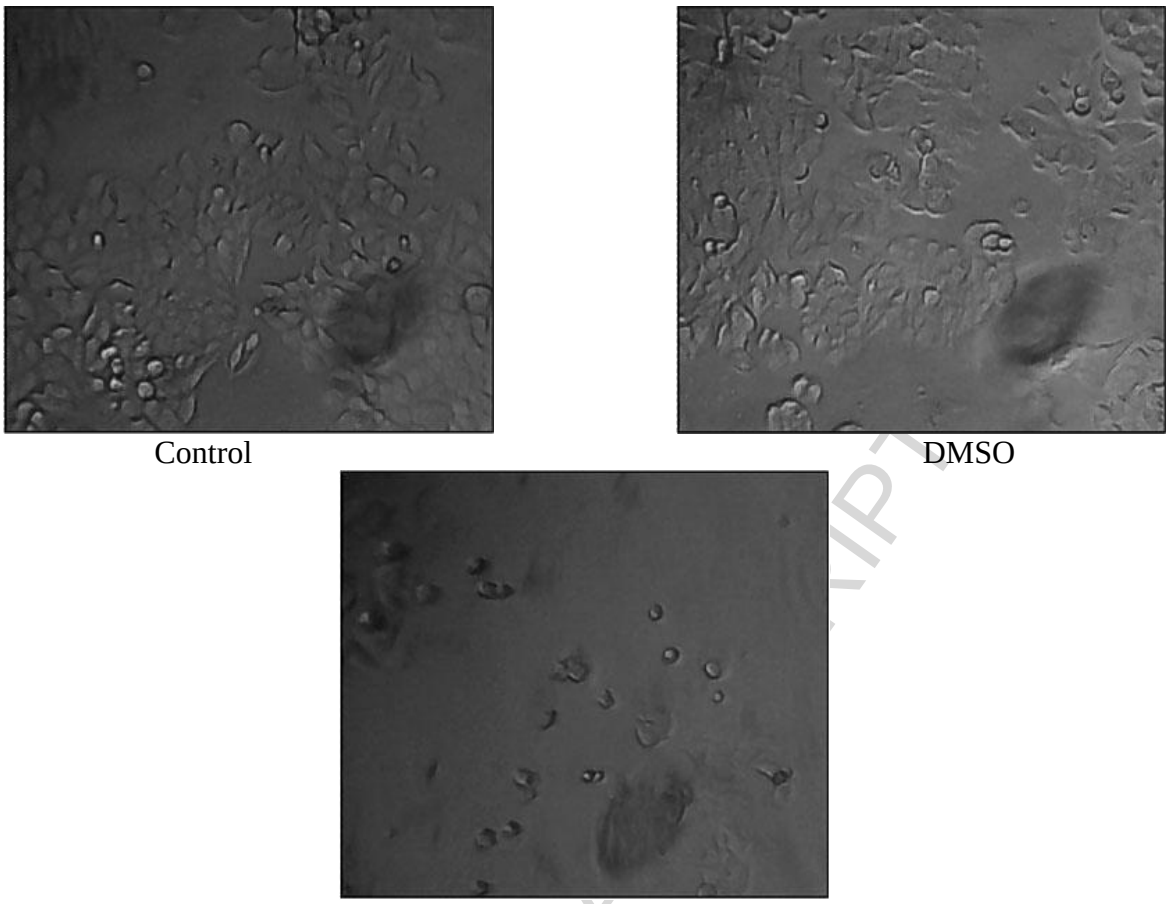

Figure 5

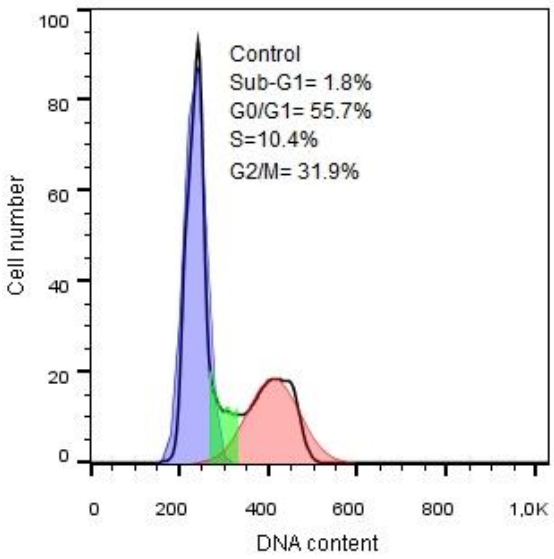

Control

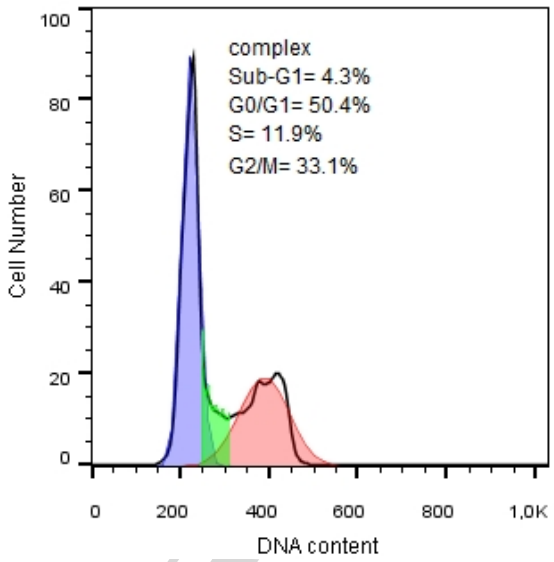

1

Figure 6

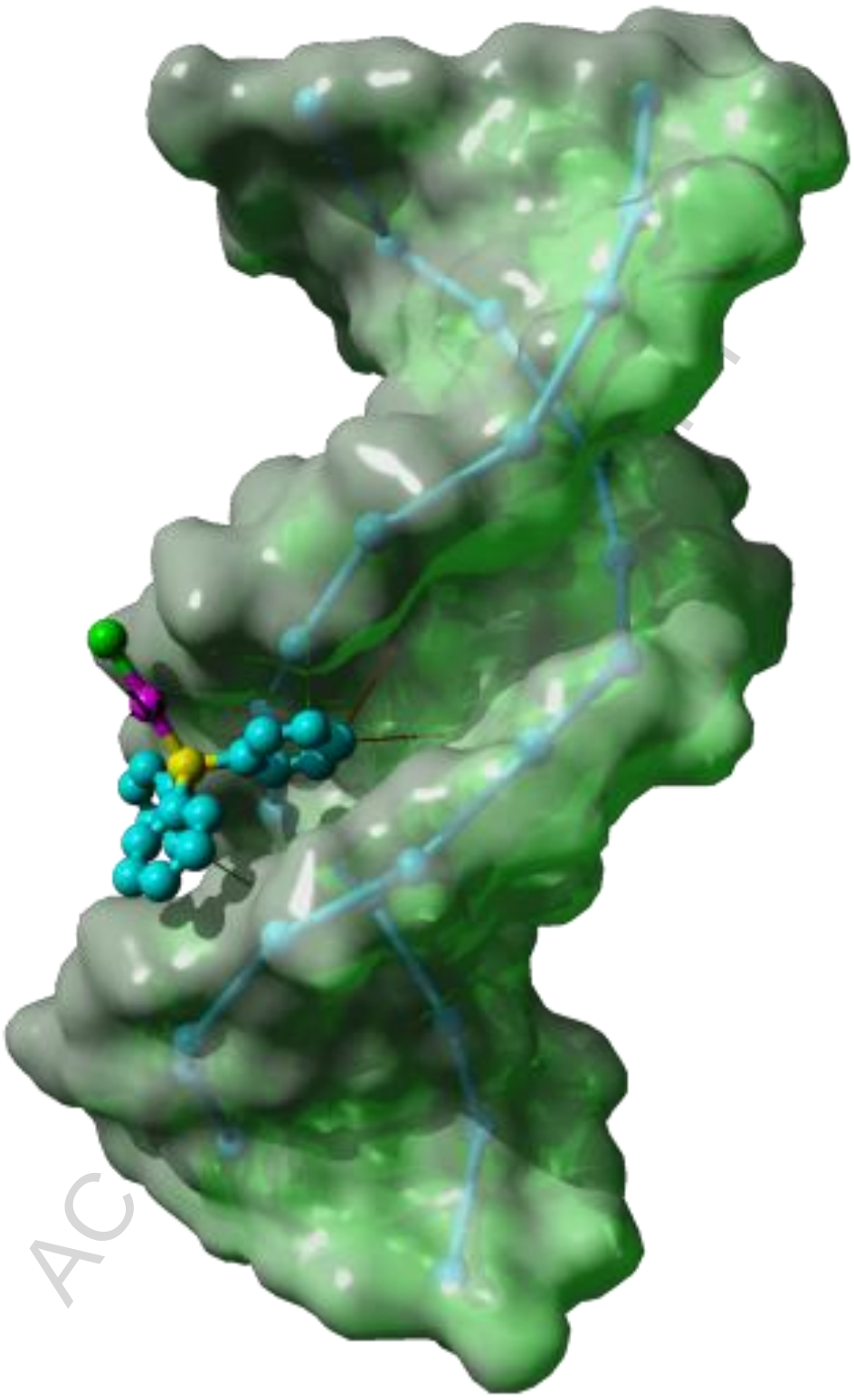

Figure 7

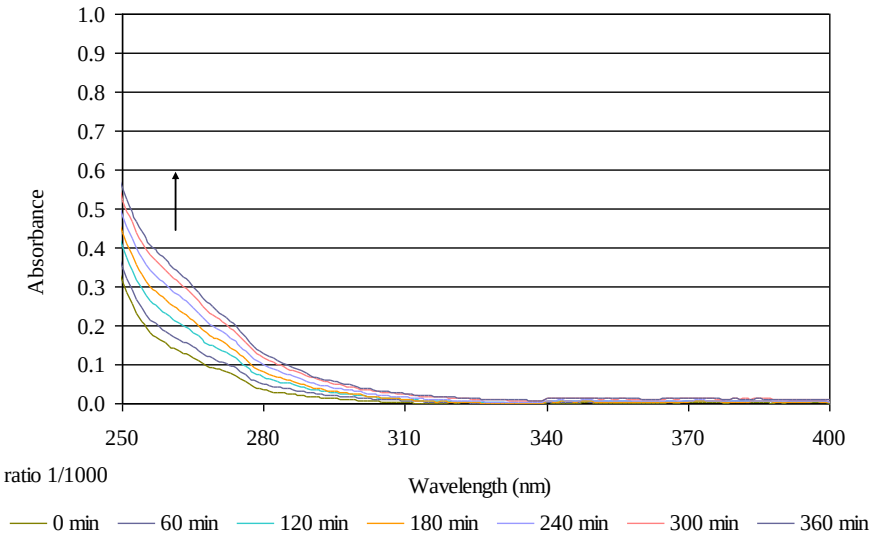

(A)

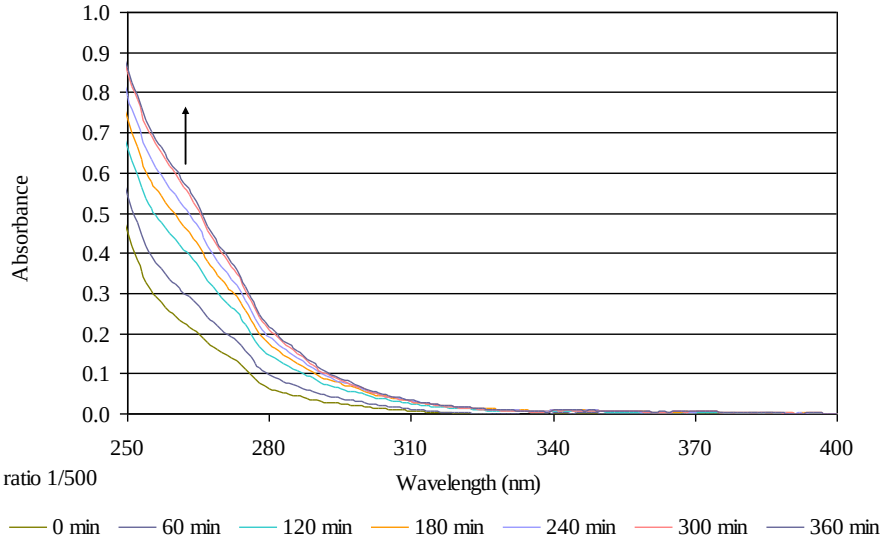

(B)

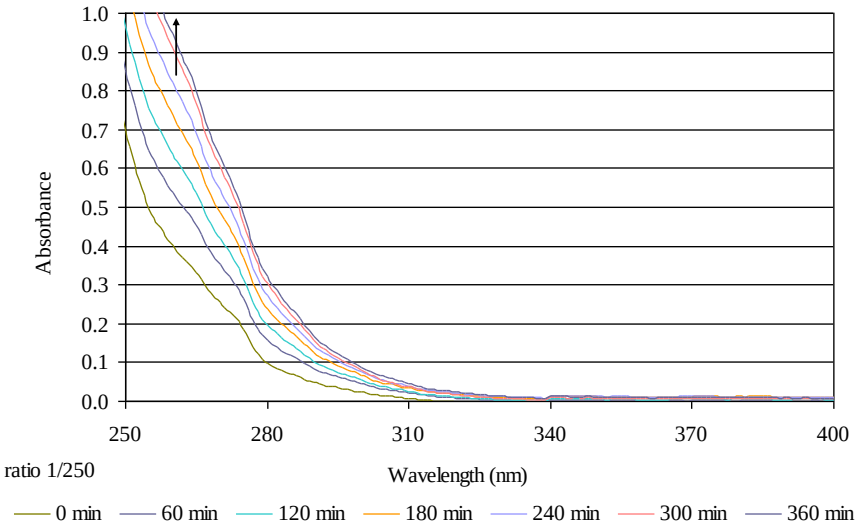

(C)

Figure 8

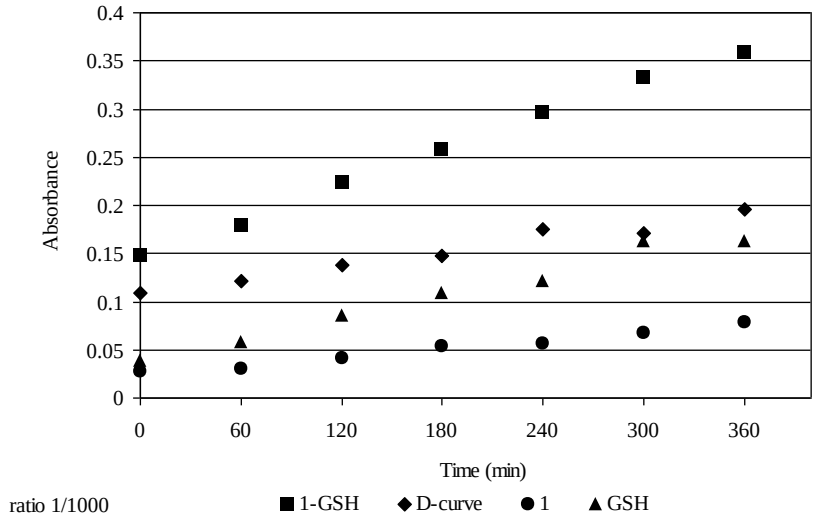

(A)

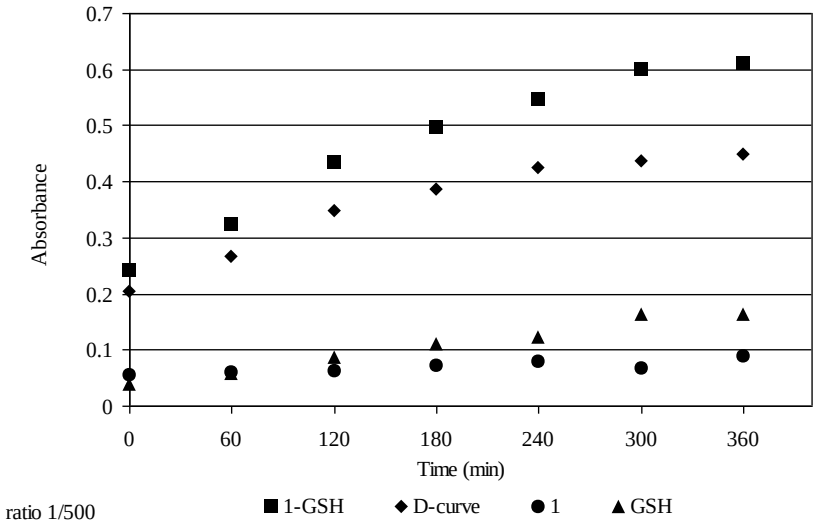

(B)

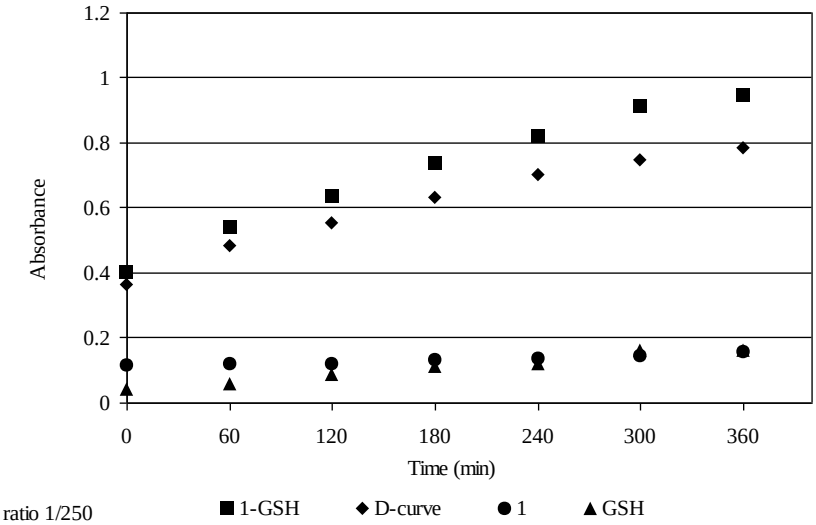

(C)

Figure 9

Graphical Abstract

Chloro(triphenylphosphine)gold(I) a forefront reagent in gold chemistry as apoptotic agent for cancer cells

M.P. Chrysouli, C.N. Banti, N. Kourkoumelis, N. Panagiotou, G.S. Markopoulos, A.J. Tasiopoulos, S.K. Hadjikakou

The activity against human breast adenocarcinoma (MCF-7) and normal human fetal lung fibroblast (MRC-5) cells of [Au(tpp)Cl] (**1**) (tpp= triphenylphosphine) was investigated. Cell cycle arrest, flow cytometry, permeabilization of the mitochondrial membrane assays and the catalytic oxidation of linoleic acid confirm the apoptotic cells death caused by **1**.

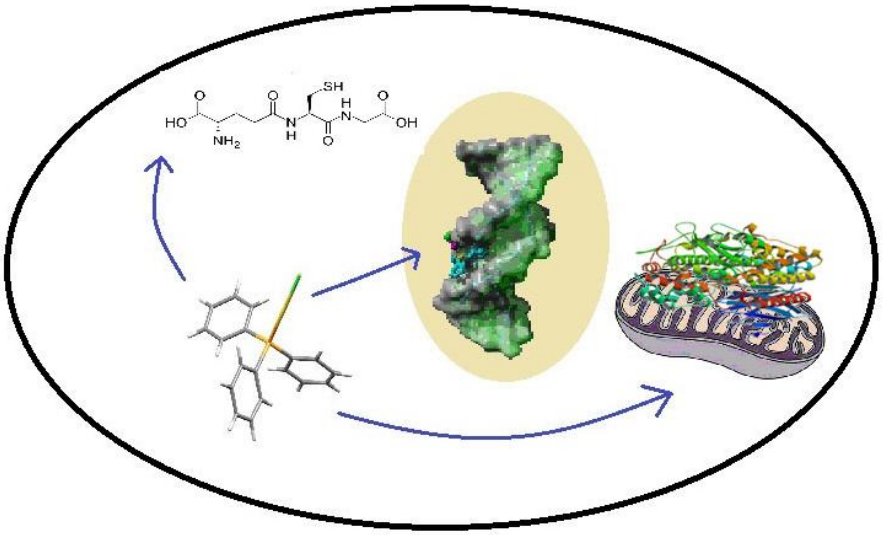

Research Highlights

Chloro(triphenylphosphine)gold(I) a forefront reagent in gold chemistry as apoptotic agent for cancer cells

M.P. Chrysouli, C.N. Banti, N. Kourkoumelis, N. Panagiotou, G.S. Markopoulos, A.J. Tasiopoulos, S.K. Hadjikakou

- Gold(I) Metallotherapeutic compound.
- Human breast adenocarcinoma cells (MCF-7) activity of the complex.
- Cell cycle arrest and permeabilization of the mitochondrial membrane tests.
- Flow cytometry assay with Annexin V-Fluorescein IsoThioCyanate, Propidium Iodide.
- Binding affinity towards Calf Thymus (CT)-DNA, and glutathione (GSH)